

Synergy of Topology and Magnetism

Chandra Shekhar[#], Sukriti Singh, Jonathan Noky, Premakumar Yanda, Avdhesh K. Sharma, Yang Zhang, Subhajit Roychowdhury and Claudia Felser

The interplay between magnetic interactions and non-trivial band structures can result various exotic physical properties, such as the substantial anomalous Hall conductivity (AHC), anomalous Nernst effect, and topological Hall effect (THE). Spin-orbit coupling and crystal symmetry are crucial in these phenomena. Our extensive study of materials, regardless of their magnetic moment, has demonstrated that significant AHC can be attained in materials featuring multiple mirror planes and considerable spin-orbit coupling. In the last three years, several materials have been studied in afore mentioned aspects and gave promising results in light of quantum anomalous Hall effect (QAHE), which is discovered at mK in some magnetic elements doped topological insulator thin films. However, achieving QAHE in bulk materials at high temperatures remains an unanswered question. Nevertheless, we found a smoking gun evidence of quantization of anomalous Hall in 3D topological magnetic layered compounds, where each layer contributes the quantized value of e^2/h at several orders of tens of Kelvin temperature. Thin films of such compounds have the ability to close the mK gap of QAHE.

Topological materials constitute a class of quantum materials characterized by gapless electronic excitations within topological electronic bands, protected by crystal symmetry [1]. These materials have garnered considerable attention due to their intriguing properties and potential for advanced technological applications. When a magnetic field is applied to a material with a flowing current, a transverse electrical current known as the classical Hall effect is observed. In certain magnetic materials, this transverse current can also occur in the absence of an external magnetic field, a phenomenon termed the anomalous Hall effect (AHE). Despite its long history, AHE remains a focus of interest due to its intricate relationship with topology and magnetism, offering deep insights into the fundamental topology of electronic structures and serving as a crucial probe for understanding magnetic order in novel materials (Figure 1).

It is noteworthy that our group has initially introduced the concept of topology and magnetism in Mn_3Sn over a decade ago. The noncollinear configurations of this material give rise to a finite Berry curvature (BC) contribution, which drives the AHE. This concept has been further developed and the idea progresses through a combination of single-crystal growth, transport measurements, and theoretical calculations, resulting in the identification of a magnetic topological family of Shandite with a Kagome lattice and Heusler compounds. The evidence for the Weyl semimetal (WSM) in $Co_3Sn_2S_2$ and the topological nodal-line semimetal in Co_2MnGa has been directly visualized through both angle-resolved photoemission spectroscopy (ARPES) and scanning tunneling microscopy (STM). In particular, $Co_3Sn_2S_2$ forms a layered structure and exhibits an intrinsic AHE and a large zero-field anomalous Nernst thermopower. This is a remarkable compound

that represents the rarest example in which AHE persists up to 100 K, despite the magnetic transition occurring at 175 K. Furthermore, the Hall conductivity per magnetic layer approaches its quantum value e^2/h , where e is the elementary charge and h is the Planck constant. Following the establishment of our concept in these compounds, we conducted research over the past three years into a number of compounds from different magnetic families in connection with topology.

Among various topological materials, itinerant ferromagnets are particularly significant within the large family where topology and magnetism are attributed to the same charge carriers. This attribute renders it relatively straightforward to tune their electronic structure and magnetism, both of which exhibit strong topological features. Depending on the crystal symmetry, either a Weyl point or nodal line forms in the band structure, acting as a source of non-zero Berry curvature (BC). This report focuses on exploring the physical properties of various topological magnets, particularly emphasizing their correlation with electronic structure. Our investigations have led to a deeper understanding of the tunability of transport properties in these systems, culminating in high anomalous Hall conductivity (AHC) at above room temperature. This can lead to find quantum anomalous Hall at room temperature. The guiding principle of crystal symmetry enhances BC distribution, significantly improving the physical properties.

Topological nodal line and Weyl magnets

ZrMnP and HfMnP crystallize in a TiNiSi-type orthorhombic structure with space group (SG) $Pnma$ (No. 62). They are itinerant ferromagnets with a Curie

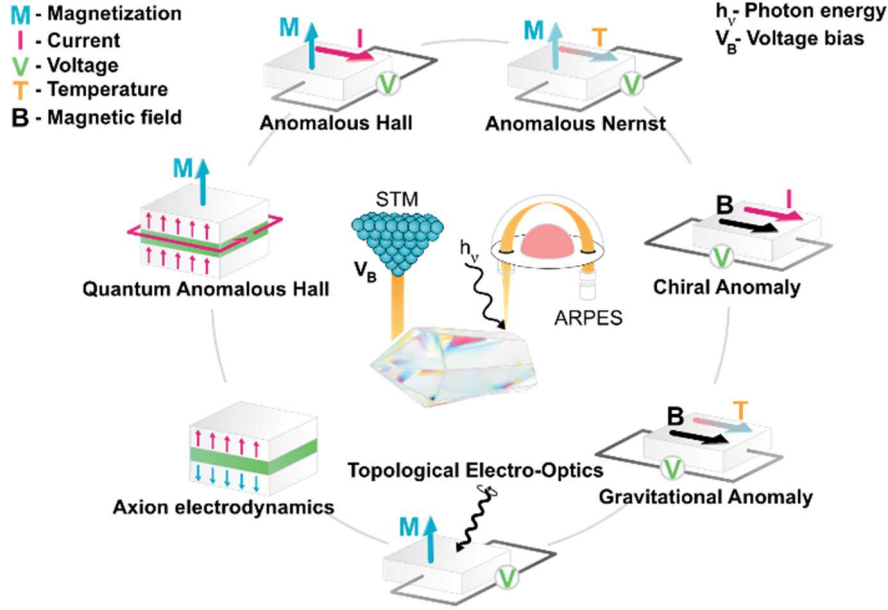


Fig. 1: Several types of experimental identification of magnetic topological materials.

temperature (T_C) of 320 K for ZrMnP and 370 K for HfMnP. Only Mn atoms contribute to the magnetism. The crystals typically exhibit needle-shaped growth along the b -axis, with well-defined facets, and pronounced magnetic anisotropy is expected. The saturation magnetization is $\sim 2.0 \mu\text{B f.u.}^{-1}$ at 2 K. The electronic band structure indicates that these compounds possess Dirac nodal lines, which are protected by various mirror planes at different energies [2]. With the exception of a narrow band along the Γ - Y direction (black line), only those bands (green lines) appearing at the Fermi energy (E_F) contribute to the nodal lines (Figure 2). This occurs due to the presence of three mutually perpendicular mirror planes in the specific SG symmetry Pnma. Both compounds exhibit anomalous behavior in Hall resistivity. To obtain the anomalous Hall resistivity, the standard rule of linear fit at high magnetic fields was applied, and the resulting anomalous Hall values were converted into AHC. The estimated AHC from the measured AHE at 2 K is $2840 \Omega^{-1} \text{cm}^{-1}$ for HfMnP and $2000 \Omega^{-1} \text{cm}^{-1}$ for ZrMnP, observable up to their T_C . The position of the nodal line relative to the E_F is considered crucial. Therefore, the nodal line structure can be assumed to contribute significantly to the transport properties. In these two cases, the number of mirror planes is related to the crystal structure, while the location is material-specific. Our current investigation suggests that selecting a compound with a high AHC can be achieved by tuning the mirror symmetry inherent in various achiral space groups.

A material's physical properties are significantly influenced by the type of topological property and its proximity to the E_F . Typically, topology near the E_F has a more pronounced effect on the AHC than topology located further away. However, our recent findings suggest that AHC is determined solely by BC, independent of its distance from the E_F . This phenomenon has been termed the *extended Berry curvature effect*, validated through theoretical models and empirical examples.

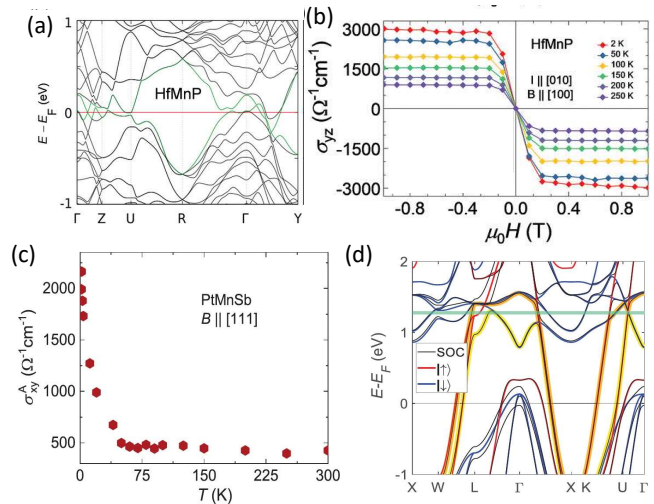


Fig. 2: (a) Band structure and (b) Anomalous Hall conductivity of HfMnP. Bands (green lines) which contribute to forming nodal-lines. (c) Anomalous Hall conductivity and (d) Band structure of PtMnSb. The two high velocity bands are highlighted in yellow and orange.

To further validate this concept, two compounds, NiMnSb and PtMnSb from the half-Heusler series, were selected for analysis. These compounds exhibit high T_C above room temperature, specifically 660 K for NiMnSb and 560 K for PtMnSb, with a magnetic moment of approximately 4.0 μ_B per formula unit at 2 K. Both compounds crystallize in the non-centrosymmetric cubic structure of the MgAgAs-type, space group $F-43m$ (No. 216), with three interpenetrating fcc lattices occupied by Ni (Pt), Mn, and Sb atoms. Single crystals of NiMnSb and PtMnSb were produced via the flux-growth method with bismuth as a flux, and NiMnSb was also grown using a dedicated laser floating zone technique (Crystal Systems Inc., Japan) to ascertain the contribution of defects to the AHC.

Both compounds exhibited anomalous behavior in Hall resistivity, with the obtained values converted into AHC. At 2 K, the AHC for PtMnSb is $2164 \Omega^{-1} \text{cm}^{-1}$, decreasing to $450 \Omega^{-1} \text{cm}^{-1}$ at 70 K. Noticeably, the AHC remains nearly constant at $427 \Omega^{-1} \text{cm}^{-1}$ from 70 K as the temperature increases to 300 K. For NiMnSb, the AHC is $\sim 90 \Omega^{-1} \text{cm}^{-1}$ at 300 K, increasing to $180 \Omega^{-1} \text{cm}^{-1}$ at 2 K, and remains nearly constant at $90 \Omega^{-1} \text{cm}^{-1}$ after 75 K, similar to PtMnSb (Figure 2). This study demonstrates that the influence of BC on AHC does not necessarily need to be close to the E_F ; the effect can extend beyond this boundary as long as the topological band remains uncontaminated by interference from other trivial bands [3].

In addition to the AHC, a distinct phenomenon known as the topological Hall effect (THE) can emerge in materials with noncoplanar spin structures. In such cases, as conduction electrons traverse localized spin moments, they can acquire a nonzero BC with finite spin chirality, which effectively acts as a magnetic field, thereby inducing THE. EuCuAs is a particularly promising candidate in this context due to its complex magnetic phase diagram below 15 K (Figure 3). This compound crystallizes in a BeZrSi-type hexagonal layered structure (space group $P63/mmc$), where Eu layers are interspaced with Cu-As layers, and undergoes a magnetic transition at 16 K. A substantial THE with a peak value of $\sim 7.4 \mu\Omega \text{cm}$ at $T = 13 \text{ K}$ (below the Néel temperature) is observed, resulting from the noncoplanar spin structure induced by the metamagnetic transition when an out-of-plane magnetic field is applied. This finding has been further validated by neutron diffraction experiments, which reveal that the spins assume a transverse conical structure during the metamagnetic transition. The observed in EuCuAs is notably higher than those reported for other frustrated magnets and noncoplanar magnetic structures [4].

HIGHLIGHTS 2024

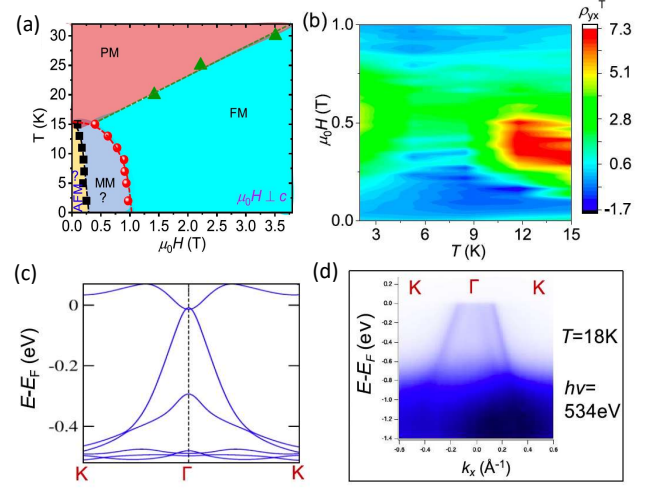


Fig. 3: EuCuAs (a) Apparent magnetic phase diagram. (b) Contour plot topological Hall effect. (c) Band structure in the paramagnetic phase. (d) ARPES intensity plot, showing topological bands.

DFT analysis confirms the presence of a single pair of Weyl points in the ferromagnetic phase of EuCuAs, highlighting the critical role of magnetism in shaping the band structure and facilitating the realization and customization of unique transport properties, including a pronounced AHC and a significant negative magnetoresistance (MR) below the saturation field.

Weyl points (WPs), which are always found in pairs with opposite chirality, arise as a result of either time-reversal symmetry (TRS) or inversion symmetry breaking, or both. When inversion symmetry is broken, a minimum of two pairs of WPs is typically generated. Conversely, when TRS is broken, the minimum number of pairs is reduced to one. Ideally, for a material to be classified as a WSM, these WPs should be located at the E_F without the interference of any other trivial bands. However, this ideal scenario is not always realized. Upon evaluating numerous systems, EuCd₂As₂ has been identified as an optimal candidate for a WSM. This compound adopts a layered structure, characterized by triangular Eu layers that separate the Cd₂As₂ layers, and crystallizes in the space group $P-3m1$.

Typically, an antiferromagnetic (AFM) ordering state is observed in this system below $\sim 9 \text{ K}$. However, an intrinsic ferromagnetic (FM) phase can be stabilized with a T_C of $\sim 26 \text{ K}$ by adjusting the level of band filling during synthesis. DFT calculations suggest that the compound exhibits a Dirac semimetal state with a single Dirac node near the E_F in the out-of-plane configuration. This state can transition into a Weyl semimetal featuring only two WPs, provided that the C_3 rotational symmetry is maintained in the spin configuration (Figure 4).

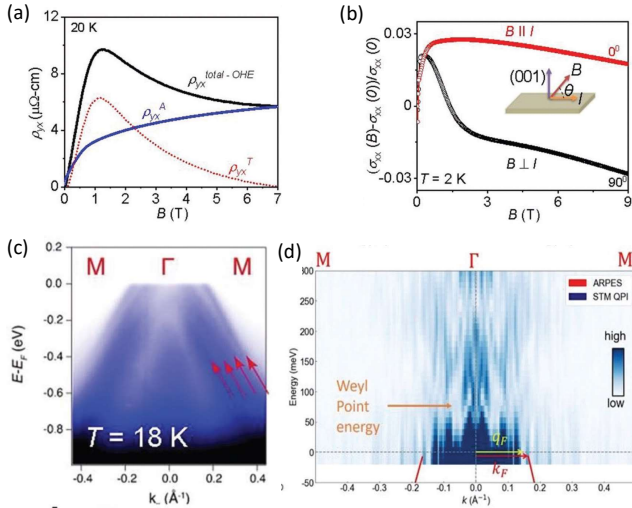


Fig. 4: EuCd_2As_2 (a) Decoupling of total Hall resistivity to anomalous Hall resistivity and topological Hall resistivity. (b) Magnetoconductivity for $B \perp I$ and $B \parallel I$ configurations. (c) ARPES intensity plots along the Γ - M direction. (d) Energy-momentum linecut of the quasiparticle interference along the Γ - M .

ARPES measurements have revealed significant differences in the band structure below and above the T_C , particularly evident in the energy bands' splitting due to FM fluctuations. The distance between the two Weyl points is approximately 0.05 \AA , a resolution challenging to achieve with ARPES. Additionally, the Weyl points are situated above the E_F , rendering them undetectable by ARPES. The utilization of Fourier transform scanning tunneling spectroscopy and visualization of quasiparticle interference enables mapping this phenomenon. Despite the expected double value, the measured maximum scattering vector at the E_F equals the Fermi wavevector, confirming the predominant scattering between the bulk bands and states near the Γ point, specifically the Weyl bands [5].

Toward 2D to 3D quantum anomalous Hall effect

While a combination of topology, SOC and magnetization can facilitate the generation of significant AHC at temperatures above room temperature, the additional Hall conductivity contribution via charge transfer between the magnetic layers restricts the achievement quantization. Nonetheless, progress in this area has been driven by the discovery of topological insulators (TIs). TIs can host QAH states when doped with magnetic elements such as Cr or V in (Bi, Sb, Te) [6]. The mechanism of perfect quantization can be understood by considering a single chiral conducting channel with a Chern number C equal to 1. However, the QAH states in these systems are typically observable only at mK

temperatures. The Chern number C in such multilayer configurations can be tuned by adjusting the thickness or the magnetic Cr doping concentration. While these studies provided proof of concept for the realization of QHA insulators with tunable C numbers, stabilization of QHA states to higher temperatures in magnetically doped films remains a significant challenge in practice, given the necessary complex dopant engineering. To maintain the stability of QAHE states at even higher temperatures, additional material design strategies are required to further mitigate the impact of dopant-induced disorder.

In order to address this challenge, further exploration of QAHE has been conducted in the intrinsic magnetic TI MnBi_2Te_4 , with observations made above the mK. In light of the stacking of magnetic multilayers of TIs and the tunability of C in MnBi_2Te_4 , an efficient approach has been developed to realize high- C states in $\text{MnBi}_2\text{Te}_4/\text{hBN}$ multilayer heterostructures. The stacking of n layers of MnBi_2Te_4 films with $C = 1$, interspersed with hBN monolayers, results in a high- C multilayer structure that exhibits n chiral edge modes (Figure 5). In this configuration, the total Hall conductivity can be defined as $\sigma_{xy} = C \frac{e^2}{h} \frac{1}{d}$, where d is the distance between two stacked layers. The individual layers of MnBi_2Te_4 are effectively separated, exhibiting the properties of Hall insulators with minimal interference with neighboring layers. A significant future objective is to investigate the potential for extending these concepts, with the aim of achieving the realization of a 3D quasi-quantized AHE with chiral surface states. 3D compounds in which the ferromagnetic layers are well-defined and separated by nonmagnetic spacer layers have already been reported [7]. Two such prototype ferromagnetic compounds, $\text{Co}_3\text{Sn}_2\text{S}_2$ and MnAlGe have been identified as potential candidates for further

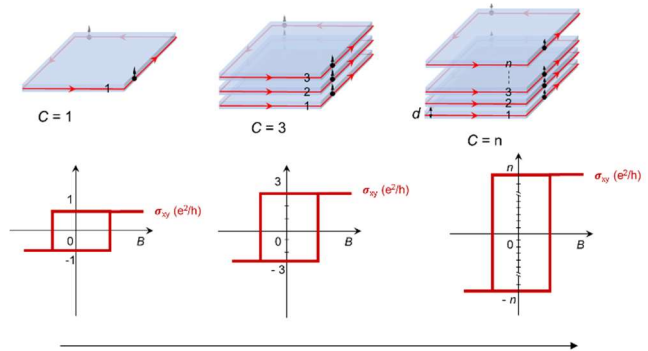


Fig. 5: Design principle of 2D to 3D quantum anomalous Hall effect using the concept of high Chern number C .

investigation to ascertain the applicability of the high-C number quasi-quantized AHE states concept (Figure 6). Here, the spins of the Co and Mn atoms are aligned in a ferromagnetic manner out of plane within each layer, and these layers are separated by a nonmagnetic spacer layer [8].

In the past three years, several promising magnetic topological materials have been designed and investigated using a combination of theoretical and experimental approaches. These developments have underscored the extraordinary potential of this class of materials advancing fundamental scientific knowledge and driving technological innovation. Interestingly, the individual magnetic layers within the bulk form of the compounds such as $\text{Co}_3\text{Sn}_2\text{S}_2$ and MnAlGe appear to satisfy the requisite conditions for achieving the QAHE. It can be anticipated that thin films or monolayers of these compounds have the potential to achieve QAHE at temperatures that are significantly higher than those previously observed. Moreover, a multitude of magnetic topological materials has been postulated from the pool of magnetic materials [9]. Depending on the type of magnetic interactions and topological gap, a variety of physical phenomena can be realized, including axion and Chern physics, which require further investigation. In this regard, a defect-free intrinsic magnetic topological material, similar to Mn_2BiTe_4 , is a good option. To achieve the long-term objective, the various experimental techniques for identifying magnetic topological materials will be employed, as illustrated in Figure 1.

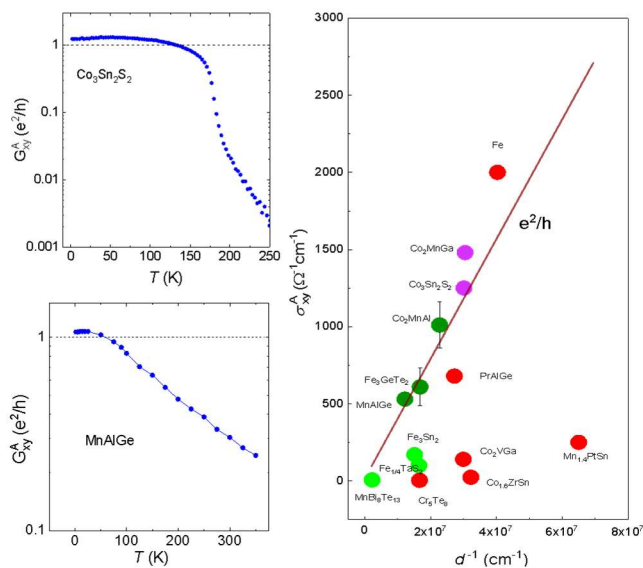


Fig.6: Some of the measured examples of compounds to realize 3D quantum anomalous Hall effect. Topological magnetic compounds are very close to quantum value (e^2/h) line.

External Cooperation Partners

Hans-Henning Klauss (TU Dresden); Vidya Madhavan (University of Illinois Urbana, USA); Vladimir Strocov (PSI, Switzerland); Emmanuel Guilmeau (CNRS, France).

References

- [1]* *Progress and Prospects in Magnetic Topological Materials*, B. A. Bernevig, C. Felser, H. Beidenkopf, *Nature* **603** (2022) 41, <https://doi.org/10.1038/s41586-021-04105-x>
- [2]* *Anisotropic Nodal-Line-Derived Large Anomalous Hall Conductivity in ZrMnP and HfMnP*, S. Singh, J. Noky, S. Bhattacharya, P. Vir, Y. Sun, N. Kumar, C. Felser, C. Shekhar, *Adv. Mater.* **33** (2021) 2104126, <https://doi.org/10.1002/adma.202104126>
- [3]* *Extended Berry Curvature Tail in Ferromagnetic Weyl Semimetals NiMnSb and PtMnSb*, S. Singh, A.-G. Page, J. Noky, S. Roychowdhury, M. G. Vergniory, H. Borrmann, H.-H. Klauss, C. Felser, C. Shekhar, *Adv. Sci.* **11** (2024) 2404495, <https://doi.org/10.1002/advs.202404495>
- [4]* *Interplay between Magnetism and Topology: Large Topological Hall Effect in an Antiferromagnetic Topological Insulator, EuCuAs*, S. Roychowdhury, K. Samanta, P. Yanda, B. Malaman, M. Yao, W. Schnelle, E. Guilmeau, P. Constantinou, S. Chandra, H. Borrmann, M. G. Vergniory, V. Strocov, C. Shekhar, C. Felser, *J. Am. Chem. Soc.* **145** (2023) 12920, <https://doi.org/10.1002/advs.202207121>
- [5]* *Anomalous Hall Conductivity and Nernst Effect of the Ideal Weyl Semimetallic Ferromagnet EuCd₂As₂*, S. Roychowdhury, M. Yao, K. Samanta, S. Bae, D. Chen, S. Ju, A. Raghavan, N. Kumar, P. Constantinou, S. N. Guin, N. C. Plumb, M. Romanelli, H. Borrmann, M. G. Vergniory, V. N. Strocov, V. Madhavan, C. Shekhar, C. Felser, *Adv. Sci.* **10** (2023) 2207121, <https://doi.org/10.1002/advs.202207121>
- [6] C.-Z. Chang et al. *Experimental observation of the quantum anomalous Hall effect in a magnetic topological insulator*, *Science* **340** (2013)167, <https://doi.org/10.1126/science.1234414>
- [7] Y. J. Jin, R. Wang, B. W. Xia, B. B. Zheng, H. Xu, *Three-dimensional quantum anomalous Hall effect in ferromagnetic insulators* *Phys. Rev. B* **98** (2018) 081101, <https://doi.org/10.1103/PhysRevB.98.081101>
- [8]* *2024 roadmap on 2D topological insulators*, Bent Weber, F. R. Menges, J. Gooth, C. Felser, C. Shekhar et al. *J. Phys. Mater.* **7** (2024) 022501, <https://doi.org/10.1088/2515-7639/ad2083>
- [9] Y. Xu, L. Elcoro, Z.-D. Song, B. J. Wieder, M. G. Vergniory, N. Regnault, Y. Chen, C. Felser, B. A. Bernevig *Nature* **586** (2020) 702, <https://doi.org/10.1038/s41586-020-2837-0>

chandra.shekhar@cpfs.mpg.de